

# Dalton Transactions

Accepted Manuscript



This article can be cited before page numbers have been issued, to do this please use: N. Stavgianoudaki, M. Siczek, T. Lis, G. Lorusso, M. Evangelisti and C. J. Milios, *Dalton Trans.*, 2019, DOI: 10.1039/C9DT00440H.



This is an Accepted Manuscript, which has been through the Royal Society of Chemistry peer review process and has been accepted for publication.

Accepted Manuscripts are published online shortly after acceptance, before technical editing, formatting and proof reading. Using this free service, authors can make their results available to the community, in citable form, before we publish the edited article. We will replace this Accepted Manuscript with the edited and formatted Advance Article as soon as it is available.

You can find more information about Accepted Manuscripts in the [author guidelines](#).

Please note that technical editing may introduce minor changes to the text and/or graphics, which may alter content. The journal's standard [Terms & Conditions](#) and the ethical guidelines, outlined in our [author and reviewer resource centre](#), still apply. In no event shall the Royal Society of Chemistry be held responsible for any errors or omissions in this Accepted Manuscript or any consequences arising from the use of any information it contains.

## A decanuclear $[\text{Dy}^{\text{III}}_6\text{Zn}^{\text{II}}_4]$ cluster: a $\{\text{Zn}^{\text{II}}_4\}$ rectangle surrounding an octahedral $\{\text{Dy}^{\text{III}}_6\}$ single molecule magnet

 Received 00th January 20xx,  
Accepted 00th January 20xx

 Nikoleta Stavgianoudaki,<sup>a</sup> Milosz Siczek,<sup>b</sup> Tadeusz Lis,<sup>b</sup> Giulia Lorusso,<sup>c</sup> Marco Evangelisti<sup>c</sup> and Constantinos J. Milios<sup>\*a</sup>

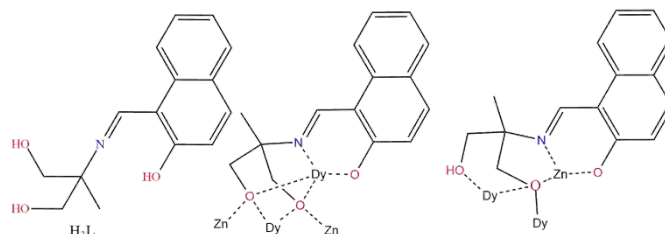
DOI: 10.1039/x0xx00000x

www.rsc.org/

**An octahedral  $\{\text{Dy}^{\text{III}}_6\}$  cage within a diamagnetic  $\{\text{Zn}^{\text{II}}_4\}$  rectangle is reported, with magnetic relaxation studies revealing single-molecule magnet behaviour for the complex under zero external dc field with  $U_{\text{eff}} = 43$  K and  $\tau_0 = 1 \times 10^{-5}$  sec.**

The field of lanthanide-based molecular magnetic materials has witnessed a vast growth over the last few years, due to the deeper understanding of the fundamental parameters that govern the magnetic behaviour of the  $4f$  centres. Especially for single molecule magnets (SMMs) or single-ion magnets (SIMs), *i.e.* molecules that are able to retain their magnetism once magnetized at low temperatures upon removal of the external magnetic field,<sup>[1]</sup> employment of  $4f$  centres has led to exceptional magnetic properties, due to both the magnitude of the spin, as well as the spin-orbit coupling based magnetic anisotropy that the  $4f$  species possess.<sup>[2]</sup> Furthermore, for Dy-based SMMs/SIMs the uniaxial magnetic anisotropy of the Dy atoms plays a crucial role in enhancing the energy barrier,  $U_{\text{eff}}$ , needed for the re-orientation of the magnetisation, and thus molecular nanomagnets with  $U_{\text{eff}}$  values over 1000 K, and blocking temperatures as high as 60 K have been reported,<sup>[3]</sup> with the best SMM/SIM being the recently reported organometallic complex  $[(\text{Cp}^{\text{iPr5}}\text{Dy}(\text{Cp}^*))^+ (\text{Cp}^{\text{iPr5}} = \text{penta-isopropylcyclopentadienyl})$  with an  $U_{\text{eff}}$  value of  $\sim 2210$  K and a blocking temperature of  $\sim 80$  K.<sup>[4]</sup> On the other hand, regarding mixed-metal  $3d-4f$  heterometallic complexes as SMM candidates, the situation seems to differ; despite the ongoing research for the construction and characterization of  $3d-4f$  SMMs, the energy barrier for such species remains rather low

compared to  $4f$  species, with  $[\text{Co}_2\text{Dy}(\text{L}^{\text{Br}})_2(\text{H}_2\text{O})]\text{NO}_3$  ( $\text{L}^{\text{Br}} = 2,2',2''\text{-}(((\text{nitrilotris}(\text{ethane-2,1diyl}))\text{tris}(\text{azanediy}))\text{tris}(\text{methylene}))\text{tris}(\text{-4-bromophenol}))$ ) holding the record of  $U_{\text{eff}} = 600$  K,<sup>[5]</sup> *i.e.*  $\sim 1/4$  of the highest  $U_{\text{eff}}$  reported so far for the best lanthanide SIM/SMM. Such a discrepancy may be attributed to either weak (and most commonly antiferromagnetic) interactions between the  $3d$  and  $4f$  metal centres, leading to low lying split sublevels, or to the perturbation of the  $4f$  local magnetic field due to random transversal secondary magnetic fields created by the nearby paramagnetic metal ions, resulting in quantum tunnelling of the magnetization and, thus, faster magnetic relaxation.<sup>[6]</sup> Recently we embarked on a project of constructing heterometallic  $\text{Zn}^{\text{II}}\text{-Ln}^{\text{III}}$  clusters and investigating their magnetic properties, as a means of: i) protecting the  $4f$ -centres from the influence of  $3d$  paramagnetic centres and ii) employing a diamagnetic  $3d$  metal atom for structural stability and diversity of the products.<sup>[7]</sup> Herein we report our latest finding regarding a decanuclear  $[\text{Zn}^{\text{II}}_4\text{Dy}^{\text{III}}_6]$  complex upon employment of the Schiff-base ligand 2-( $\beta$ -naphthalideneamino)-2-hydroxymethyl-1-propanol,  $\text{H}_3\text{L}$  (Scheme 1). The reaction of  $\text{Zn}(\text{OAc})_2 \cdot 2\text{H}_2\text{O}$ ,  $\text{Dy}(\text{NO}_3)_3 \cdot 5\text{H}_2\text{O}$  and  $\text{H}_3\text{L}$  in MeOH in 1:1:1 ratio under solvothermal conditions, and in the presence of base  $\text{NEt}_3$ , gave complex  $[\text{Dy}_6\text{Zn}_4\text{O}_2(\text{L})_2(\text{HL})_2(\text{OAc})_8(\text{CH}_3\text{O})_4(\text{H}_2\text{O})_2] \cdot 4\text{MeOH}$  (1.4MeOH) in good yield, which was characterized by means of X-ray single crystal crystallography.<sup>§</sup>



Scheme 1. The ligand and its coordination modes in 1.

<sup>a</sup> Department of Chemistry, The University of Crete, Voutes 71003, Herakleion, Greece. E-mail: [kamil@uoc.gr](mailto:kamil@uoc.gr)

<sup>b</sup> Faculty of Chemistry, University of Wrocław, Joliot-Curie 14, Wrocław 50-383, Poland.

<sup>c</sup> Instituto de Ciencia de Materiales de Aragón (ICMA), CSIC – Universidad de Zaragoza, 50009 Zaragoza, Spain.

† Footnotes relating to the title and/or authors should appear here.

Electronic Supplementary Information (ESI) available: Full details of the experimental microanalyses and crystallographic data. See DOI: 10.1039/x0xx00000x

Complex **1** crystallizes in the triclinic P-1 space group (Figure 1, top). Its metallic core consists of a diamagnetic  $\{Zn^{II}_4\}$  rectangular unit of  $\sim 6.12 \times 6.42$  Å dimensions, surrounding a central magnetic  $\{Dy^{III}_6\}$  slightly “squeezed” octahedron (Figure 1, bottom). The basal  $Dy^{III}$  ions ( $Dy_2, Dy_2', Dy_3, Dy_3'$ ) placed are located  $\sim 3.49$  and  $\sim 5.64$  Å apart, while the axial  $Dy^{III}$  centres ( $Dy_1, Dy_1'$ ) are found  $\sim 1.73$  Å above and below the basal plane.

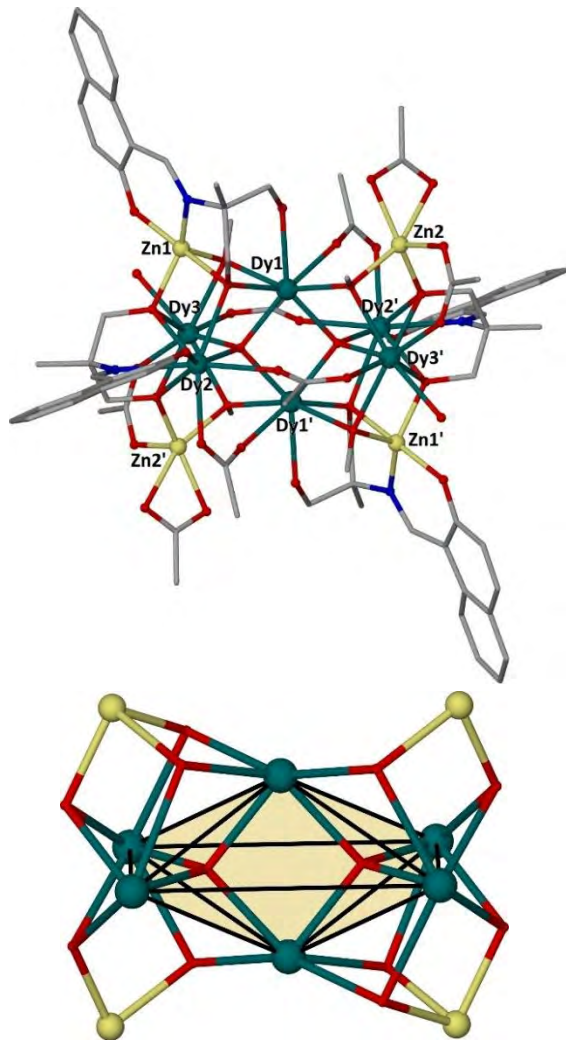


Figure 1. The crystal structure of **1** (top) and its  $\{Dy^{III}_6Zn^{II}_4\}$  metallic core (bottom) highlighting the  $\{Dy^{III}_6\}$  octahedron. Colour code:  $Zn^{II}$  = yellow,  $Dy^{III}$  = dark-green, O = red, N = blue, C = grey. H-atoms and solvate molecules are omitted for clarity

The six metallic centres of the octahedron are held by a combination of two central  $\mu_4-O^{2-}$  bridges, four monoatomic methoxide bridges, four  $\mu-\kappa^1O:\kappa^1O'$  acetates and four ligands adopting two coordination modes; two of them are found in the doubly deprotonated form,  $HL^{2-}$ , with a  $\mu_3-\kappa^3O:\kappa^1N:\kappa^1O':\kappa^1O''$  coordination mode, while the remaining two are fully deprotonated,  $L^{3-}$ , adopting a  $\mu_4-\kappa^3O:\kappa^3O':\kappa^1N:\kappa^1O''$  coordination fashion. The linkage of the two metallic sub-units occurs *via* i) the deprotonated ligands found in the molecule, ii) the four methoxide groups, and iii) two  $\mu-\kappa^1O:\kappa^1O'$  acetate groups. Finally, two chelate acetates and two terminal water molecules fill the

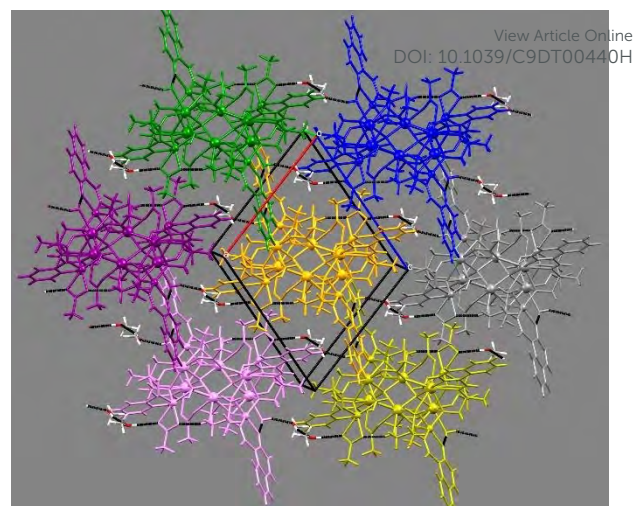


Figure 2. Crystal packing of **1**, highlighting the intermolecular H-bonds (black bold dotted lines). Each colour corresponds to an individual molecule of **1**.

coordination environment of the metallic centres. All Zn centres are five-coordinate adopting square pyramidal geometry (for  $Zn_2/Zn_2'$ ,  $\tau=0.160$ ), and severely twisted square pyramidal/trigonal bipyramidal geometry (for  $Zn_1/Zn_1'$ ,  $\tau=0.546$ ). Regarding the 4f centers, their ideal geometries were found upon performing SHAPE analysis<sup>[8]</sup>:  $Dy_2$  and  $Dy_3$  are eight-coordinate with square antiprismatic ( $D_{4d}$ ) geometry (SAPR-8:  $S(\delta_i, \theta_i)=0.958$  and  $S(\delta_i, \theta_i)=1.056$ , for  $Dy_2$  and  $Dy_3$ , respectively), while  $Dy_1$  is seven-coordinate with distorted capped trigonal prismatic geometry ( $C_{2v}$ ) ( $S_{(\delta_i, \theta_i)} = 11.476$  for CTP) (Figs. S1-S2). Finally, the  $\{Dy^{III}_6\}$  octahedron deviates slightly from the ideal octahedral geometry (CSHM = 10.649). In the crystal lattice, the molecules pack forming layers stabilized mainly by intermolecular H-bonds between the decanuclear species and the solvate methanol molecules (Figure 2).

DC magnetic susceptibility measurements were performed on **1** in the 2 – 300 K temperature range under an applied magnetic field of 0.1 T, and the results are plotted as  $\chi_M T$  vs.  $T$  in Figure 3, with the isothermal magnetisation ( $M$  vs.  $H$ ) curves shown in the

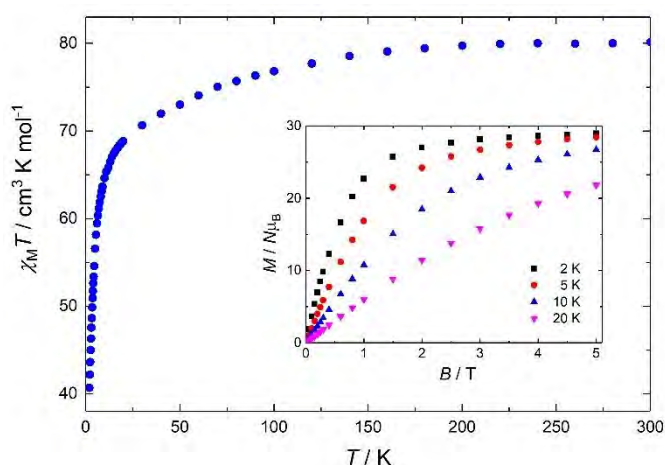


Figure 3. Plot of  $\chi_M T$  vs.  $T$  for **1** in the 2 – 300 K temperature range, under an applied field of 0.1 T. Inset:  $M$  vs.  $B$  for **1** in the 0 – 5 T and 2.0 – 20.0 K field and temperature ranges.



inset. The room-temperature  $\chi_M T$  value of  $81.2 \text{ cm}^3 \text{ mol}^{-1} \text{ K}$  is slightly smaller than the theoretical value of  $85.0 \text{ cm}^3 \text{ mol}^{-1} \text{ K}$  expected for six  $\text{Dy}^{\text{III}}$  ions ( $S = 5/2, L = 5, J = 15/2, {}^6H_{15/2}, g_J = 4/3$ ). Upon cooling, the  $\chi_M T$  product remains practically unchanged until  $\sim 150 \text{ K}$ , below which steadily decreases reaching  $41.05 \text{ cm}^3 \text{ mol}^{-1} \text{ K}$  at  $2 \text{ K}$ , possibly suggesting the presence of weak antiferromagnetic interactions within the cluster (a Curie-Weiss analysis gave  $\vartheta = -2.9 \text{ K}$ ) and/or depopulation of the  $\text{Dy}^{\text{III}}$  Stark sub-levels. The isothermal magnetization versus  $B$  plots increase rapidly, reaching values of  $29.2$  and  $28.5 N_{\mu\text{B}}$  at  $5 \text{ T}$ , for  $T = 2$  and  $5 \text{ K}$ , respectively, significantly lower than the theoretical value of  $\sim 60 N_{\mu\text{B}}$  for a hexanuclear  $[\text{Dy}^{\text{III}}_6]$  complex; this is mainly attributed to the presence of magnetic anisotropy and to the depopulation of the Stark sublevels.<sup>[9]</sup>

Given: i) the large remaining magnetic moment, even at  $2 \text{ K}$ , and ii) the square antiprismatic geometry of the  $\text{Dy}2$  and  $\text{Dy}3$  centres (and their symmetry related) that promotes suitable charge distribution with axial anisotropy on the  $\text{Dy}^{\text{III}}$  centres,<sup>[10]</sup> we investigated the AC dynamic magnetic properties of **1**. The measurements show temperature and frequency ( $f$ ) dependent fully-formed in-phase,  $\chi_M'$ , and out-of-phase,  $\chi_M''$ , signals, under zero-applied DC field and a  $3.5 \text{ AC}$  field oscillating at various frequencies, in the temperature range between ca.  $3$  and  $15 \text{ K}$  (Figure 4). This behaviour seems to indicate slow relaxation of the magnetization, which is typical for a SMM.

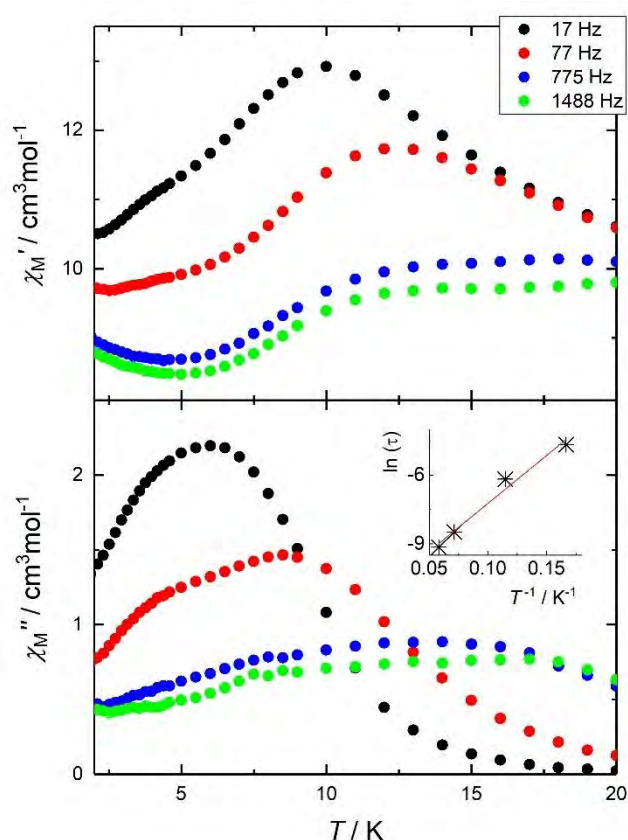


Figure 4. (Top) In-phase,  $\chi_M'$ , and out-of-phase (bottom),  $\chi_M''$ , signals for **1** at various frequencies in the  $17 - 1488 \text{ Hz}$  range. Inset: Arrhenius fit of the effective time constants.

The main feature is a cusp in the in-phase component that occurs at approximately  $10.0 \text{ K}$  for  $f = 17 \text{ Hz}$ , accompanied by a cusp in the out-of-phase component at somewhat lower temperature (Figure 4). Effective time constants can be obtained from the reciprocal angular frequency at maximum absorption. As typical of a thermal activation process, the zero-field relaxation times so obtained can be approximated by the Arrhenius law  $\tau = \tau_0 \exp(U_{\text{eff}}/k_B T)$ , where  $\tau = (2\pi f)^{-1}$ ,  $\tau_0$  is an attempt frequency and  $U_{\text{eff}}$  an effective energy barrier. The results are presented in the inset of Figure 4, affording  $U_{\text{eff}} = 43 \text{ K}$  and  $\tau_0 = 1 \times 10^{-5} \text{ sec}$ . The AC susceptibility reveals that the magnetic relaxation is particularly complex in **1**, since at least another (secondary) relaxation pathway can be spotted at somewhat lower temperature than that of the main feature. In order to visualize the orientation of the anisotropy axis for each  $\text{Dy}^{\text{III}}$  ion present in **1**, we employed the electrostatic model reported by Chilton *et al.*, which is based on electrostatic energy minimization for the prediction of the ground state magnetic anisotropy axis,<sup>[11]</sup> assuming that in the absence of high symmetry the ground-state of  $\text{Dy}^{\text{III}}$  ions is a doublet along the anisotropy axis with  $m_J = \pm 15/2$ .<sup>[12]</sup> Following this approach, the ground state magnetic anisotropy axes in **1** were found to form three pairs from the symmetry-related  $\text{Dy}$  centres (Figure 5); for  $\text{Dy}1(\text{Dy}1')$  the axis is tilted towards the  $\mu_4\text{-O}1$  oxide atom, and towards  $\text{O}2$  belonging to a monoatomic methoxide bridge and  $\text{O}2\text{F}$  belonging to bridging acetate group. For  $\text{Dy}2(\text{Dy}2')$  the axis is pointing towards the  $\mu_4\text{-O}1$  oxide atom and towards  $\text{O}2\text{B}(\text{O}2\text{B}')$  from a deprotonated aromatic hydroxyl group, while for  $\text{Dy}3(\text{Dy}3')$  the axis is tilted towards the  $\mu_4\text{-O}1'$  oxide atom and the  $\text{O}2\text{D}'$  atom of a bridging acetate group.

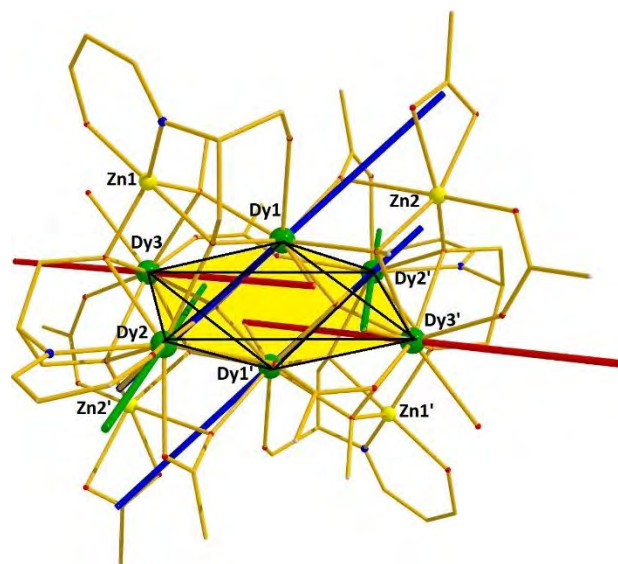


Figure 5. Ground state magnetic anisotropy axis for the  $\text{Dy}$  centers present in **1**.

## Conclusions

In conclusion, in this work we present the synthesis and characterisation of a novel decanuclear  $[\text{Dy}^{\text{III}}_6\text{Zn}^{\text{II}}_4]$  cluster, upon employment of the Schiff-base ligand  $2-(\beta-$

naphthalideneamino)-2-hydroxymethyl-1-propanol, H<sub>3</sub>L, with the cluster's topology describing a {Zn<sup>II</sup><sub>4</sub>} rectangle surrounding a {Dy<sup>III</sup><sub>6</sub>} octahedron. Furthermore, investigation of the magnetic properties, revealed possible SMM behaviour with  $U_{\text{eff}} = 43$  K and  $\tau_0 = 1 \times 10^{-5}$  sec. To the best of our knowledge, complex **1** represents the first example of a decanuclear [Dy<sup>III</sup><sub>6</sub>Zn<sub>4</sub>] single molecule magnet.

Synthetic efforts are currently underway in order to isolate more Zn-4f clusters, as a means of investigating the effect of the diamagnetic ions on the magnetic behaviour of the 4f centres.

### Conflicts of interest

The authors wish to declare no conflicts of interest.

### Acknowledgements

GL and ME thank MINECO for funding (MAT2015-68204-R).

### Notes and references

† Footnotes relating to the main text should appear here. These might include comments relevant to but not central to the matter under discussion, limited experimental and spectral data, and crystallographic data.

§ Crystal data for **1**: 4MeOH: C<sub>83</sub>H<sub>112</sub>Dy<sub>6</sub>N<sub>4</sub>O<sub>40</sub>Zn<sub>4</sub>, M = 3042.24, triclinic, space group P-1, a = 13.591 (3) Å, b = 13.807 (3) Å, c = 14.560 (3) Å, α = 80.22 (2)°, β = 69.83 (2)°, γ = 77.36 (2)°, V = 2489.2 (10) Å<sup>3</sup>, Z = 1, T = 80 K, R1 (I > 2σ) = 0.037 and wR2 (all data) = 0.074 for 37200 reflections collected, 10607 observed reflections (I > 2σ(I)) of 14033 (Rint = 0.039) unique reflections and 634 parameters, GOF = 1.02. CCDC reference number: 1892887.

- For representative reviews on SMMs see: G. Aromi and E. K. Brechin, *Struct. Bond.*, 2006, **122**, 1; R. Bircher, G. Chaboussant, C. Dobe, H. U. Güdel, S. T. Ochsenein, A. Sieber and O. Waldman, *Adv. Funct. Mater.*, 2006, **16**, 209; D. Gatteschi and R. Sessoli, *Angew. Chem., Int. Ed.*, 2003, **42**, 268; G. Christou, D. Gatteschi, D. N. Hendrickson and R. Sessoli, *MRS Bull.*, 2000, **25**, 66; C. J. Milios and R. E. P. Winpenny, *Struct. Bond.*, 2015, **164**, 1; L. Sorace, C. Benelli and D. Gatteschi, *Chem. Soc. Rev.*, 2011, **40**, 3092; X.-Y. Wang, C. Avendaño and K. R. Dunbar, *Chem. Soc. Rev.*, 2011, **40**, 3213; L. R. Piquer and E. C. Sañudo, *Dalton Trans.*, 2015, **44**, 8771; R. A. Layfield, *Organometallics*, 2014, **33**, 1084; L. K. Thompson and L. N. Dawe, *Coord. Chem. Rev.*, 2015, **289**, 13; S. Demir, I.-R. Jeon, J. R. Long and T. D. Harris, *Coord. Chem. Rev.*, 2015, **289**, 149; P. Happ, C. Plenck and E. Rentschler, *Coord. Chem. Rev.*, 2015, **289**, 238; G. A. Craig and M. Murrie, *Chem. Soc. Rev.*, 2015, **44**, 2135.
- See for example: R. Sessoli and A. K. Powell, *Coord. Chem. Rev.*, 2009, **253**, 2328; D. N. Woodruff, R. E. P. Winpenny and R. A. Layfield, *Chem. Rev.*, 2013, **113**, 5110; J. D. Rinehart and J. R. Long, *Chem. Sci.*, 2011, **2**, 2078; Y.-N. Guo, G.-F. Xu, Y. Guo and J. Tang, *Dalton Trans.*, 2011, **40**, 9953; P. Zhang, Y.-N. Guo and J. Tang, *Coord. Chem. Rev.*, 2013, **257**, 1728; Y.-N. Guo, G.-F. Xu, P. Gamez, L. Zhao, S.-Y. Lin, R. Deng, J. Tang and H.-J. Zhang, *J. Am. Chem. Soc.*, 2010, **132**, 8538; Y.-N. Guo, G.-F. Xu, W. Wernsdorfer, L. Ungur, Y. Guo, J. Tang, H.-J. Zhang, L. F. Chibotaru and A. K. Powell, *J. Am. Chem. Soc.*, 2011, **133**, 11948; B. M. Day, F.-S. Guo and R. A. Layfield, *Acc. Chem. Res.*, 2018, **51**, 1880; S. T. Liddle and J. van Slageren, *Chem. Soc. Rev.*, 2015, **44**, 6655; A. F. R. Kilpatrick, F.-S. Guo, B. M. Day, A. Mansikkamäki, R. A. Layfield and F. G. N. Cloke, *Chem. Commun.*, 2018, **54**, 7085; M. Feng and M.-L. Tong, *Chem. Eur. J.*, 2018, **24**, 7574.
- Y.-S. Ding, N. F. Chilton, R. E. P. Winpenny and Y.-Z. Zheng, *Angew. Chem. Int. Ed.* 2016, **55**, 16071; D. S. Krylov, F. Liu, S. M. Avdoshenko, L. Spree, B. Weise, A. Waske, A. U. B. Wolter, B. Buechner and A. A. Popov, *Chem. Commun.* 2017, **53**, 7901; Y.-C. Chen, J.-L. Liu, L. Ungur, J. Liu, Q.-W. Li, L.-F. Wang, Z.-P. Ni, L. F. Chibotaru, X.-M. Chen and M.-L. Tong, *J. Am. Chem. Soc.*, 2016, **138**, 2829; S. K. Gupta, T. Rajeshkumar, G. Rajaraman and R. Murugavel, *Chem. Sci.*, 2016, **7**, 5181; Y.-S. Meng, L. Xu, J. Xiong, Q. Yuan, T. Liu, B.-W. Wang and S. Gao, *Angew. Chem. Int. Ed.* 2018, **57**, 1; A. B. Canaj, M. K. Singh, C. Wilson, G. Rajaraman and M. Murrie, *Chem. Commun.*, 2018, **54**, 8273; F.-S. Guo, B. M. Day, Y.-C. Chen, M.-L. Tong, A. Mansikkamaeki and R. A. Layfield, *Angew. Chem. Int. Ed.* 2017, **56**, 11445; C. A. P. Goodwin, F. Ortu, D. Reta, N. F. Chilton and D. P. Mills, *Nature*, 2017, **548**, 439
- F.-S. Guo, B. M. Day, Y.-C. Chen, M.-L. Tong, A. Mansikkamäki and R. A. Layfield, *Science*, 2018, **362**, 1400.
- J.-L. Liu, J.-Y. Wu, G.-Z. Huang, Y.-C. Chen, J.-H. Jia, L. Ungur, L. F. Chibotaru, X.-M. Chen and M.-L. Tong, *Scientific Reports*, 2015, **5**, 16621.
- M. A. Palacios, S. Titos-Padilla, J. Ruiz, J. M. Herrera, S. J. A. Pope, E. K. Brechin and E. Colacio, *Inorg. Chem.*, 2014, **53**, 1465; A. Bhunia, M. T. Gamer, L. Ungur, L. F. Chibotaru, A. K. Powell, Y. Lan, P. W. Roesky, F. Menges, C. Riehn and G. Niedner-Schatteburg, *Inorg. Chem.*, 2012, **51**, 9589.
- N. Stavgiannoudaki, M. Siczek, T. Lis, R. Inglis and C. J. Milios, *Chem. Commun.*, 2016, **52**, 343.
- M. Llunell, D. Casanova, J. Girera, P. Alemany and S. Alvarez, SHAPE, version 2.0, Barcelona, Spain 2010.
- J. K. Tang, I. Hewitt, N. T. Madhu, G. Chastanet, W. Wernsdorfer, C. E. Anson, C. Benelli, R. Sessoli and A. K. Powell, *Angew. Chem., Int. Ed.*, 2006, **45**, 1729; S. Osa, T. Kido, N. Matsumoto, N. Re, A. Pochaba and J. Mrozinski, *J. Am. Chem. Soc.*, 2004, **126**, 420.
- N. Ishikawa, M. Sugita, T. Ishikawa, S.-Y. Koshihara and Y. Kaizu, *J. Am. Chem. Soc.* 2003, **125**, 8694; M. A. Aldamen, J. M. Clemente-Juan, E. Coronado, C. Mart-Gastaldo, A. Gaitarino, *J. Am. Chem. Soc.* 2008, **130**, 8874; G. Zhou, T. Han, Y.-Song Ding, N. F. Chilton, and Y.-Zhen Zheng, *Chem. Eur. J.* 2017, **23**, 1.
- N. F. Chilton, D. Collison, E. J. L. McInnes, R. E. P. Winpenny and A. Soncini, *Nature Commun.*, 2013, **4**, 2551.
- See for example: S. K. Langley, N. F. Chilton, L. Ungur, B. Moubaraki, L. F. Chibotaru and K. S. Murray, *Inorg. Chem.*, 2012, **51**, 11873; G. Cucinotta, M. Perfetti, J. Luzon, M. Etienne, P.-E. Car, A. Caneschi, G. Calvez, K. Bernot, and Roberta Sessoli, *Angew. Chem. Int. Ed.*, 2012, **51**, 1606; Y.-N. Guo, G.-F. Xu, W. Wernsdorfer, L. Ungur, Y. Guo, J. Tang, H.-J. Zhang, L. F. Chibotaru and A. K. Powell, *J. Am. Chem. Soc.*, 2011, **133**, 11948; N. F. Chilton, S. K. Langley, B. Moubaraki, A. Soncini, S. R. Batten and K. S. Murray, *Chem. Sci.*, 2013, **4**, 1719; F. Tuna, C. A. Smith, M. Bodensteiner, L. Ungur, L. F. Chibotaru, E. J. L. McInnes, R. E. P. Winpenny, D. Collison and R. A. Layfield, *Angew. Chem. Int. Ed.*, 2012, **51**, 6976.

**A decanuclear  $[\text{Dy}^{\text{III}}_6\text{Zn}^{\text{II}}_4]$  cluster: a  $\{\text{Zn}^{\text{II}}_4\}$  rectangle surrounding an octahedral  $\{\text{Dy}^{\text{III}}_6\}$  single molecule magnet**

New Article Online  
DOI: 10.1039/C9DT00440H

Nikoleta Stavgianoudaki, Milosz Siczek, Tadeusz Lis, Giulia Lorusso, Marco Evangelisti and Constantinos J. Milios

The synthesis, structure and magnetic relaxation properties of a decanuclear  $[\text{Dy}^{\text{III}}_6\text{Zn}^{\text{II}}_4]$  complex are reported.

